Textile & Leather Review

ISSN 2623-6281 | www.tlr-journal.com | 10.31881/TLR

A Multi-Objective Optimization and Robustness Evaluation Framework for Heterogeneous Logistics Systems Based on Spatio-Temporal Extended Linear Programming and Stochastic Risk Perception

Jiyan Zhang, Jinyuan Hui, Jinhui Zhang, Chen Xu

How to cite: Zhang J, Hui J, Zhang J, Xu C. A Multi-Objective Optimization and Robustness Evaluation Framework for Heterogeneous Logistics Systems Based on Spatio-Temporal Extended Linear Programming and Stochastic Risk Perception. Textile & Leather Review. 2026; 9:2655-2680. https://doi.org/10.31881/TLR.2026.2655

How to link: https://doi.org/10.31881/TLR.2026.2655

Published: 25 April 2026

A Multi-Objective Optimization and Robustness Evaluation Framework for Heterogeneous Logistics Systems Based on Spatio-Temporal Extended Linear Programming and Stochastic Risk Perception

Jiyan Zhang*, Jinyuan Hui, Jinhui Zhang, Chen Xu

School of Computer and Information Technology, Northeast Petroleum University, Daqing 163318, China

*15203917970@163.com

Article

https://doi.org/10.31881/TLR.2026.2655

Published 25 April 2026

ABSTRACT

Addressing the dual challenges of efficiency and risk resilience in large-scale heterogeneous resource scheduling, this study constructs an integrated computational decision-making framework combining trend forecasting, dynamic programming, and stochastic simulation. The research first proposes a five-dimensional multi-model prediction framework, employing non-stationary programming algorithms such as logistic regression, Grey prediction, and learning curves to perform parameter identification for core variables including future logistics scale, costs, and system reliability. For large-scale cargo transshipment tasks, a Time-Space Extended Linear Programming (TELP) model is developed. Through a two-level optimization strategy combining outer-layer time enumeration and inner-layer linear programming, the Pareto frontier between transportation duration and economic cost is successfully decomposed, identifying optimal equilibrium solutions under heterogeneous collaboration modes. To address random disturbances during system operation, a robustness assessment mechanism based on Conditional Value at Risk (CVaR) is introduced. Combined with Monte Carlo simulation, this quantifies the impact of tail risks on schedule duration. Finally, by designing an adaptive material classification and allocation algorithm alongside a reliability-aware inventory optimization model, the expected value loss of the system is reduced by 67.6% under service level constraints, while optimizing the environmental load caused by emergency dispatching. The universal computational paradigm established in this study provides precise mathematical tools for stability evaluation and automated scheduling of complex systems under extreme conditions.

KEYWORDS

spatio-temporal extended linear programming, five-dimensional forecasting framework, conditional value at risk

INTRODUCTION

In ultra-large-scale logistics systems engineering, constructing a scheduling framework that balances high throughput with low operational costs while maintaining robustness under dynamic conditions represents a core challenge at the intersection of computer science and operations research. Particularly when confronting non-stationary, long-horizon planning tasks, systems often face dual pressures from high-dimensional parameter fluctuations and sudden structural failures. Traditional single-modal transportation evaluation frameworks often struggle to handle dynamic coordination among large-scale heterogeneous resources and lack effective capture of extreme "tail risks" in risk quantification. Previous research has predominantly focused on static linear weighting or path search under ideal conditions, neglecting the nonlinear cost evolution driven by technological iteration and the cascading impact of failure risks on supply chains.

To bridge these gaps, this study introduces a groundbreaking innovation: a five-dimensional multi-model prediction framework integrating physical constraints with data-driven insights. It develops a spatio-temporally extended linear programming algorithm featuring two-stage optimization logic, bridging the gap from deterministic planning to stochastic risk response. The overall research approach follows a logical sequence of parameter deduction, multimodal scheduling optimization, CVaR-based robustness assessment, and lifecycle assurance optimization. It aims to enhance decision quality under irrational disturbances by searching for optimal solution sets within complex decision spaces through multi-objective evolutionary iteration.

To rigorously validate the universality and computational efficiency of the proposed framework, this paper selects the Earth-Moon Logistics System for Lunar Base Construction as a representative case study. This scenario represents a typical "extreme logistics" problem characterized by ultra-long time horizons, massive heterogeneous resource coordination, and strict reliability constraints. It should be noted that while a transport capacity of 100 million tons represents an extremely high per-capita volume from a global perspective, during the early stages of lunar construction, large-scale lunar regolith reinforcement facilities and fully enclosed industrial-grade life support systems are essential to cope with the extreme radiation environment. According to some deep-space exploration studies, the mass density of infrastructure required to sustain long-term extraterrestrial settlements is far higher than that on Earth. Specifically, the construction of a lunar colony involves the transportation of approximately 100 million tons of materials, requiring a collaborative system comprising conventional rockets (high speed but high cost) and space elevators (low cost but limited throughput and technological immaturity). The complex trade-offs between these heterogeneous transport

modes and the random disturbances such as launch failures and cable disasters provide an ideal testbed for the proposed Time-Space Extended Linear Programming (TELP) and CVaR-based robustness models.

Following this case-driven methodology, the remainder of this paper is organized as follows: We first construct the five-dimensional forecasting framework to estimate key parameters for 2050. Subsequently, we develop the TELP model to derive the Pareto frontier between time and cost for mixed transportation strategies. To address operational risks, a robustness assessment mechanism based on Monte Carlo simulation and CVaR is introduced, accompanied by a material classification and allocation strategy. Finally, we establish a reliability-aware inventory optimization model to manage lifecycle resource assurance under environmental constraints.

MODELS

Data Sources and Processing

To construct the evaluation model in an objective and scientifically grounded manner, we compile data through 2025 from authoritative sources in the aerospace domain (e.g., NASA and SpaceX) to support parameterization and cost estimation. The resulting data categories and their intended uses are summarized in Table 1.

Table 1. Data categories and intended uses

Type	Objective
Rocket payload capacity, launch frequency, and cost[1-2]	The rockets annual capacity, how long it would take to achieve 100 million tons, and the total cost.
Elevator Data[3]	Simulation of Elevator Energy Consumption and Operational Costs.
Material Composition and Logistical Support[4-8]	Estimate the water consumption of residents and the population structure after migration.
Environmental Impact and Grid Carbon Intensity[2] [9]	The Environmental Impact of Rocket Fuel Combustion and the Carbon Intensity of the Power Grid.
Physical Constants and Orbital Parameters[10]	Obtain certain parameters to carry out a simulation of contingencies.

Five-Dimensional Multi-Model Forecasting Framework

The transportation system required for constructing a Moon Colony represents a long-horizon, strongly non-stationary planning problem: environmental regulations, technological iteration, the energy structure, and monetary purchasing power are all expected to change substantially by 2050. Consequently, historical statistics available through 2026 cannot be used directly to parameterize a 2050 assessment; otherwise, transport capacity and costs may be systematically under- or over-estimated[11-12]. To ground the subsequent models

in realistic future scenarios, we develop a five-dimensional, multi-model forecasting framework that projects the five most sensitive input variables emission frequency; unit cost and capacity; reliability and emissions; monetary purchasing power; and energy and operating costs separately, and outputs the 2050 parameter table X_{2050} . Five-dimensional multi-model forecast framework is shown in figure 1.

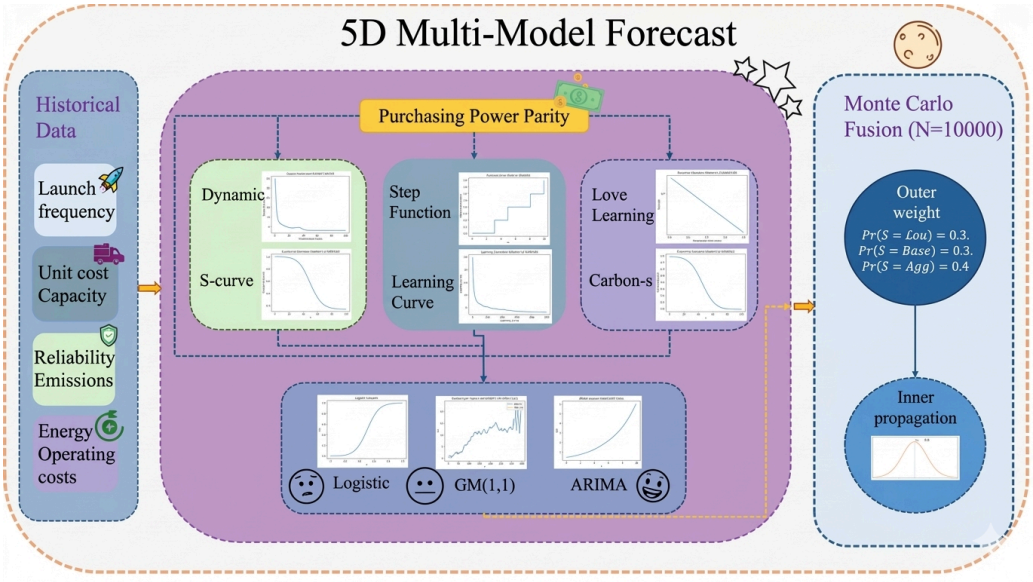

Figure 1. Five-dimensional multi-model forecast framework

(1) Unified Variable Preprocessing

We standardize all collected variables prior to forecasting. First, we harmonize the timeline by aligning all series to an annual scale and defining the index $t = 1990, ..., 2025$; missing years are imputed using linear interpolation or a neighboring-mean approach. Next, we standardize units by converting mass to tons/year and costs to USD/kg. We then construct derived variables, including the annual launch frequency $N(t)$, the cumulative launch volume $X(t) = \sum_{\tau \le t} N(\tau)$, and a reliability metric used to evaluate rocket launch success rates. Finally, we enforce physically plausible bounds on predicted variables (e.g., success rate ≤ 0.99 , cost $\ge$ baseline, and share $\in [0, 1]$) to prevent unrealistic extrapolations during simulation[13].

(2) FD Multi-Model Prediction Framework Data Forecast for 2050

Dimension One: Economic Benchmark Standardization

To eliminate the effects of inflation, we standardize monetary values reported in different years to a common purchasing-power basis. Drawing on NIAC reports, we adjust the cost terms—including rocket unit cost and

the elevator construction and operating costs—for inflation and purchasing-power normalization. All costs are then converted to 2050 USD using a long-term inflation assumption r .

$$FV = PV(1+r)^n, n = 2050 - 2003 \tag{1}$$

Dimension Two: Annual Launch Frequency Forecast

Rocket launch frequency is a primary driver of annual throughput, yet it cannot increase indefinitely and is ultimately constrained by practical system limits. Using historical launch data from 1990 to 2025, we construct a boundary forecasting model that combines three approaches to project the annual launch frequency in 2050.

Conservative scenario. We treat launch activity as capacity-constrained growth with system limit K and model is using a logistic curve:

$$N(t) = \frac{K}{1 + Ae^{-r(t-t_0)}} \tag{2}$$

Aggressive scenario. To capture the acceleration associated with the commercial-space boom from 2015 to 2025, we adopt the grey forecasting model GM(1,1), which is sensitive to short-term exponential trends, as an upper bound[14-15]. Given the advantages of GM(1,1) in short-term extrapolation with small sample sizes, we use it solely as an “upper bound estimate” within our five-dimensional forecasting framework to capture the exponential nature of recent cost reductions in the commercial space industry, rather than as the sole tool for long-term trend forecasting. This multi-model ensemble strategy aims to balance historical inertia with technological discontinuities.

Compromise scenario. We treat the long-term trend as a slowly varying stable process and apply ARIMA/ETS to extract the trend component, yielding the baseline forecast.

Dimension Three: Unit Cost and Carrying Capacity

Given that rocket recovery has already been demonstrated, it is reasonable to assume that reusability becomes mature by 2050. As a result, scaling and reuse are expected to reduce unit cost; however, costs cannot fall to zero because a non-negligible floor remains due to propellant, ground operations, labor, and maintenance. We therefore forecast both rocket unit cost and single-launch payload capacity for 2050.

Unit cost forecast. We use a Wright learning curve:

$$C(X) = C_1 \cdot X^{-b} \tag{3}$$

$C_{\min}$ is anchored to propellant costs, with the minimum estimated ground operating cost used as a lower bound.

Payload capacity forecast. To reflect generational technology upgrades, we model the single-launch payload capacity as a step function:

$$Q(t) = Q_0 + \sum_i \Delta Q_i \cdot 1(t \geq t_i) \tag{4}$$

The single-launch cost and payload capacity estimated for each year are then fed into the boundary model in Dimension Two to obtain the 2050 single-launch cost and payload capacity under the three scenarios[16].

Dimension Four: Reliability and Environmental Impact

Reliability improves with accumulated operational experience, while the failure rate decreases according to power law. Accordingly, we adopted the Duane empirical learning model:

$$\lambda(B) = \alpha \cdot B^{-\beta} \tag{5}$$

Emissions and clean-fuel penetration. With the policy push toward carbon peaking and carbon neutrality, emissions per unit mass from rocket propulsion are expected to decline over time. We assume that the adoption of clean fuels follows an S-curve—slow growth initially, rapid uptake in the middle stage, and saturation at maturity—and define the clean-fuel share as:

$$s(t) = \frac{1}{1 + e^{-k(t - t_{mid})}} \tag{6}$$

The resulting weighted CO2 emissions per launch can then be expressed as:

$$E(t) = E_{dirty}(1 - s(t)) + E_{clean}s(t) \tag{7}$$

We then input the estimated reliability and per-launch CO2 emissions into the boundary model in Dimension Two to obtain rocket reliability and per-launch CO2 emissions in 2050 under the three scenarios[17].

Dimension Five: Energy Benchmarking and Operational Cost Forecasting

Although direct historical data for the elevator are unavailable, its marginal operating cost depends primarily on electricity prices and grid carbon intensity. We therefore forecast 2050 elevator operating costs and associated indirect emissions using projections of industrial electricity prices and grid carbon intensity.

Industrial electricity price forecast. By combining an LCOE learning curve with energy-storage system costs, we project a 2050 industrial electricity price range $[p_{\min}, p_{\max}]$. Grid carbon-intensity forecast. Similarly, we represent the decline in grid carbon intensity toward the 2050 target using an S-curve.

Elevator operating costs: Computed from energy intensity η and electricity price p :

$$c_E(2050) \approx \eta \cdot p + c_{OM} \tag{8}$$

The resulting elevator operating costs are then fed into the boundary model in Dimension Two to obtain 2050 elevator operating costs under the three scenarios. Monte Carlo Aggregate Mean: From Three Scenarios to a Single Benchmark Input.

The five-dimensional forecasting framework yields parameter sets under three scenarios, reflecting different levels of technological maturity, scale, and constraint intensity. To obtain a single benchmark parameter set that can be used directly for subsequent transportation scheduling and cost accounting under uncertainty, we employ a two-layer Monte Carlo integration scheme.

Uncertainty in the external context

Given the rapid pace of technological advancement in recent years, we adopt a mildly optimistic prior for 2050. Rather than assigning equal probability to each scenario, we treat the scenario indicator $S \in \{Con, Base, Agg\}$ as a discrete random variable and assign a slightly higher weight to the grey-model forecast:

$$Pr(S = Con) = 0.3, Pr(S = Base) = 0.3, Pr(S = Agg) = 0.4 \tag{9}$$

Inner Parameter Propagation

After completing the outer scenario sampling, we propagate uncertainty in the inner parameters by mapping fluctuations in the five-dimensional forecasted inputs to the outputs of the downstream transport model. Repeating this procedure N times and taking the average yields:

$$Y_{MC} = \frac{1}{N}\sum_{k=1}^{N} Y^{(k)} \tag{10}$$

Table 2. 2050 baseline inputs

Category	Final Data Item	2050 Composite Value	Unit
Launch Scale	Annual Launch Frequency N_{2050}	8,717	Launches/Year
Payload Capacity	Single-Mission Payload Capacity Q_{2050}	133.5	Tons per Mission
Cost	Rocket Unit Cost $c_{R,2050}$	13,689	$/kg
Success Rate	Reliability R_{2050}	0.986	-
Economic Impact	Single-Mission CO2 Emission $E_{launch,2050}$	166.5	Tons per Mission
Economic Indicator	Space Elevator Capital Expenditure, $CAPEX_{E,2050}$	29.9	$B
Elevator Operation and Maintenance	Elevator Unit Transportation Cost $c_{E,2050}$	48	$/kg

2050 baseline inputs are shown in table 2.

Time-Expanded Linear Programming Mixed Transportation Model

To address the challenge of transporting approximately 100 million tons of construction materials for a Moon Colony designed to accommodate 100,000 people, we consider three scenarios defined by the two primary decision metrics of time and cost: (a) using only the elevator; (b) using only conventional rocket launches; and (c) adopting a hybrid strategy that combines both channels. For the hybrid case, we develop a time-expanded linear programming (LP) mixed-transportation model. Time-Expanded Linear Programming Mixed Transportation Model work process workflow is summarized in Figure 2. Specifically, the model employs a two-level strategy: an outer-layer enumeration over the construction duration T and an inner-layer LP solve. This procedure generates a cost–time Pareto frontier, which is then used to identify the optimal allocation[18-19].

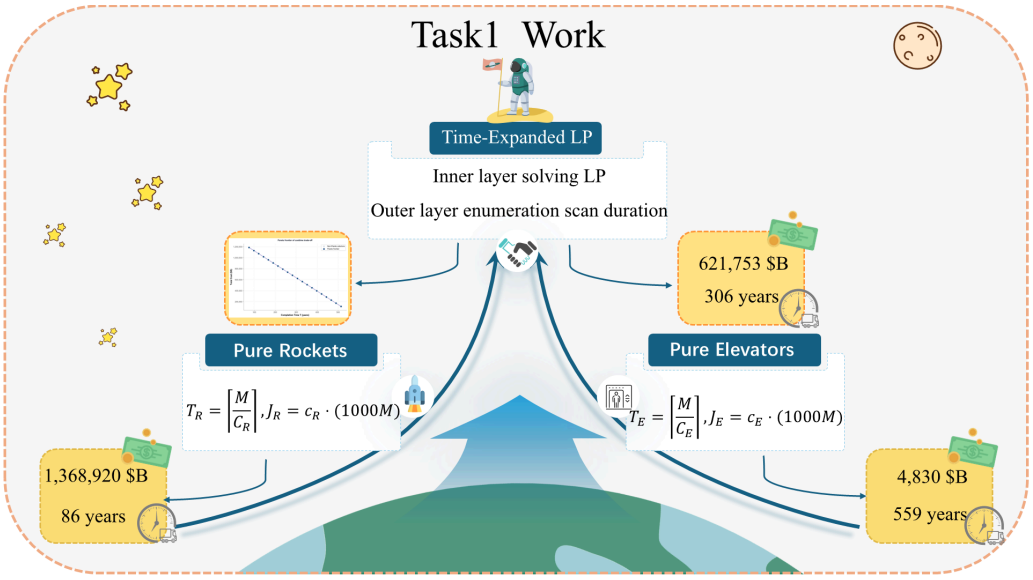

Figure 2. Time-Expanded Linear Programming Mixed Transportation Model work process

Data Processing

We first define equivalent capacity and cost parameters for each transportation channel. Let the total material demand over the construction period be M (tons). Let the rocket channel have annual transport capacity C_R and unit transport cost c_R ; the corresponding parameters for the elevator channel are C_E and c_E . To benchmark single-mode performance, we define the construction duration and total transportation cost for the pure-rocket and pure-elevator schemes as follows:

$$T_R = \left\lceil \frac{M}{C_R} \right\rceil, J_R = c_R \cdot (1000M), T_E = \left\lceil \frac{M}{C_E} \right\rceil, J_E = c_E \cdot (1000M) \tag{11}$$

If the space elevator project is delayed due to insufficient technological maturity, the system will automatically revert to “pure rocket mode.” As shown in Table 3, in the extreme sensitivity scenario where the elevator is absent, the construction period would be reduced from 306 years in the baseline scenario to 86 years (assuming sufficient transport capacity), but the total cost would skyrocket to 1,368,920 B dollars. This comparison quantifies the elevator’s core value as a low-cost corridor in long-term planning. Rockets provide high time efficiency but incur high unit costs, whereas the elevator is comparatively cost-effective yet, if used alone, could require centuries to deliver the full demand at the 10^8 -ton scale. Therefore, no single approach can serve as an engineering-feasible construction strategy. This motivates a systematic trade-off between time efficiency and cost control. Single option result is shown in table 3.

Table 3. Single option result table

Plan	Total Cost ($B)	Total Duration (Years)
space elevator system	4,830	559
conventional rockets	1,368,920	86

Time-Expanded Linear Programming Mixed Transportation Model

We establish a time expansion linear programming (LP) hybrid transportation model. First, the total time of transportation is expanded, and the construction period is divided into $t = 1, 2, ..., T$ years. Define the decision variables r_t and e_t to represent the quantity of materials transported by rockets and space elevators in year t respectively. Since the bottleneck of a single system comes from its annual throughput capacity, the annual capacity constraint is first imposed to avoid exceeding the actual transportation situation:

$$0 \le r_t \le C_R, 0 \le e_t \le C_E, \forall t \tag{12}$$

And limit the total transportation volume to meet the construction demand:

$$\sum_{t=1}^{T}(r_t + e_t) = M \tag{13}$$

Given a fixed project duration T , the system tends to allocate more volume to the lower-cost channel while satisfying the annual capacity and total-demand constraints. If T is too short and the throughput of low-cost channels is insufficient to meet demand, the remaining demand must be covered by higher-cost channels. Therefore, we formulate the inner layer as an LP to compute the minimum achievable cost under the duration constraint T . Because costs are linearly additive, the total cost is expressed as:

$$\min J(T) = \sum_{t=1}^{T}(c_R \cdot 1000 r_t + c_E \cdot 1000 e_t) \tag{14}$$

Because the construction duration T is a discrete integer variable, directly optimizing T together with the annual quotas would lead to a mixed-integer program and reduce transparency. We therefore adopt a two-tier strategy: we enumerate candidate values of T in the outer layer and solve the inner LP to obtain the

corresponding minimum cost $J(T)$. Based on the system's total throughput upper bound, the minimum feasible duration is:

$$T_{\min} = \left\lceil \frac{M}{C_R + C_E} \right\rceil \tag{15}$$

Accordingly, we perform an annual enumeration starting from $T = T_{\min}$. For each candidate T , we solve the inner LP to obtain the minimum cost $J(T)$, which yields a time–cost Pareto set:

$$P = \{(T, J(T)) \mid T = T_{\min}, T_{\min} + 1, \ldots\} \tag{16}$$

The results are shown in figure 3, which illustrates the Pareto frontier and the stacked diagram of transportation modes. The Pareto analysis reveals a pronounced nonlinear trade-off between the costly "short-duration scheme" (75 years, $1.86T) and the prolonged "minimal price scheme" (514 years, $1.14T). Based on this, we identify the "compromise balance scheme" (306 years, $622T) at the knee point of the curve, which achieves an acceptable project duration while avoiding extreme marginal costs. Pareto frontier: time vs cost & transport mix is shown in figure 3. Specifically, this inflection point is derived through a mathematical calculation that minimizes the Euclidean distance (or "minimum Manhattan distance") between the normalized time T and cost J and the ideal origin, ensuring an optimal trade-off between the two conflicting objectives.

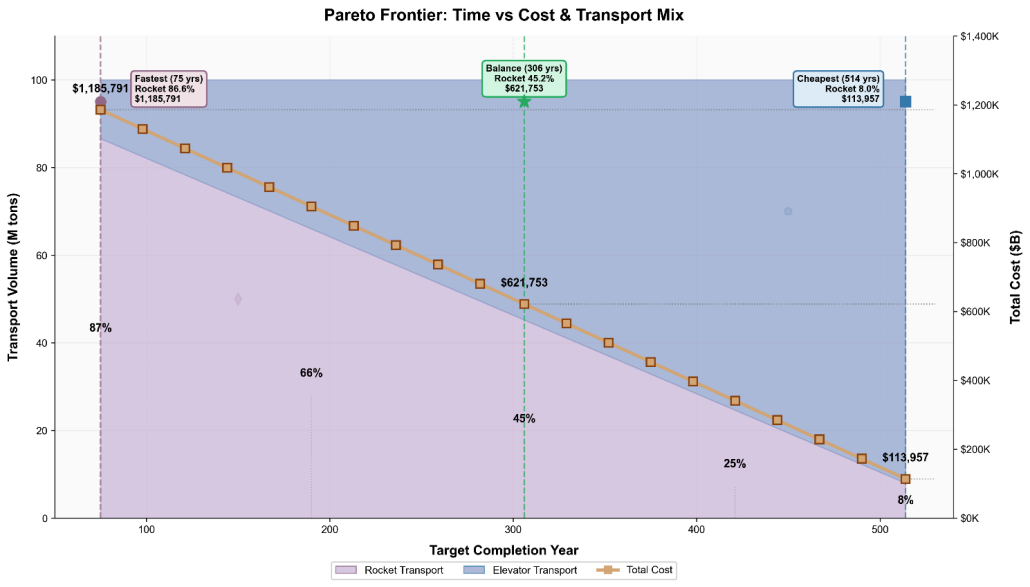

Figure 3. Pareto frontier: time vs cost & transport mix

Model Risk Assessment and Improvement

Based on the risk assessment of the time expansion linear programming hybrid transportation model, we introduce the reliability fluctuation and disaster shutdown of rockets and space elevators, expand the duration and cost from a single point value to a random variable, and use Monte Carlo scenario simulation + CVaR (95%) to depict the tail risk.

Risk assessment settings

We first use a proportional parameter for each deterministic hybrid strategy in risk assessment:

$$\rho \in [0,1], M_R = \rho M, M_E = (1-\rho)M \tag{17}$$

Then, we establish an uncertain model to evaluate the annual effective capacity and disaster shutdown of rockets and elevators. For each year (t) , two random effective factors are introduced:

Rocket reliability factor $p_R(t)$: fluctuates around the weighted average success rate and is truncated within a reasonable range to represent the effective rocket throughput of the year.

Elevator reliability factor $a_E(t)$: the effective throughput rate composed of availability and wobble factor, with annual fluctuation added.

Elevator disaster event: if "whether there is at least one disaster within the assessment window of (H) years" is taken as the index, the disaster probability is:

$$P(\geq 1) = 1 - (1-\pi_c)^H \tag{18}$$

When (H) is very large, this value will quickly approach 1. Therefore, different transportation strategies, even with different levels of elevator dependence, will exhibit approximately constant disaster probabilities and lack discrimination under the condition of "whether there has been a disaster over a long period." For this reason, we define the occurrence of a cable-failure-level system disaster with an annual probability π_c . Once it occurs, the elevator is shut down for Y_c years, and a fixed repair cost K_c is incurred. The corresponding key parameter settings are listed in Table 4.

Table 4. Risk parameter setting

Item	Value
Rocket success rate	98.6%
Elevator availability	95.1%
Wobble factor	90.0%
Effective capacity of elevator	85.6%
Disaster probability (year)	0.5%
Years of downtime	4
Repair cost ($B)	75

Although a 98.6% success rate implies that there would be approximately 122 incidents out of 8,717 launches per year, within the logistical framework of this model, we assume that future launch operations will be conducted using automated launch arrays deployed in remote, uninhabited areas or on the high seas, thereby keeping physical safety risks and negative public perception within acceptable limits.

Secondly, we simulate the real scenario by advancing year by year until the project is completed or reaches the upper limit of assessment. The upper limit is set to 600 years, because the deterministic construction period of the pure elevator scheme is approximately 559 years and may easily exceed 600 years under risk; thus, 600 years is used as the criterion for “cross-century unacceptable.”

For elevators, we perform the transportation process of “annual deduction of residual demand” for each random scenario (ω) . The effective throughput of the year is given by

$$C_R^{\omega}(t) = C_R \cdot p_R^{\omega}(t), C_E^{\omega}(t) = C_E \cdot a_E^{\omega}(t) \tag{19}$$

Annual delivery:

$$\Delta M_R(t) = \min(M_R^{rem}, C_R^{\omega}(t)), \Delta M_E(t) = \min(M_E^{rem}, C_E^{\omega}(t)) \tag{20}$$

For rocket launch, if the success rate of the current year is $p_R^{\omega}(t)$, then to deliver the “successful arrival quantity” of $\Delta M_R(t)$, the required trial quantity is:

$$M_R^{try}(t) = \frac{\Delta M_R(t)}{p_R^{\omega}(t)} \tag{21}$$

Accordingly, the annual rocket cost is charged based on the trial volume, while the elevator cost is charged based on the actual throughput. If elevators are used, the disaster recovery cost K_c is added.

In this problem, fluctuations in rocket success rates, elevator disaster shutdowns, and total loss from high-value cargo failures lead to significant skewness in the distributions of project duration and cost. Using only the expectation $E[X]$ would mask "tail extreme bad cases," while VaR only provides a threshold and does not reflect the magnitude of losses beyond it. Therefore, for each ρ , we obtain duration and cost samples $\{T(\rho,\omega_i), C(\rho,\omega_i)\}_{i=1}^{N}$ under $N = 1000$ scenarios. The outputs include $E[T]$, $E[C]$, $CVaR_{0.95}(T)$, $CVaR_{0.95}(C)$, where CVaR is computed as the tail mean exceeding $VaR_{0.95}$:

$$CVaR_{0.95}(X) = E[X \mid X \geq VaR_{0.95}(X)] \tag{22}$$

Risk Assessment Performance of the Hybrid Transportation Model

We obtain the model risk assessment results by incorporating the risk assessment into the hybrid model, as reported in Table 5. We find that the introduction of risk leads to an average increase of approximately 16%–19% in the construction period and about 1.7% in total cost. In particular, under the low-cost scheme with a low proportion of rockets, risk effects push the construction period to an unacceptable level. In addition, the original hybrid model assumes "no differentiation among goods," and the impacts of scrapping high-value goods and accident costs associated with dangerous goods are not explicitly represented. This simplification underestimates the mission risk of high-value goods in the event of rocket failure.

Table 5. Risk assessment results of the original model

Plan	Proportion of rockets (%)	Deterministic years	$E[T]$	$CVaR_{95}[T]$	Deterministic cost ($B)	$E[C]$ (B)	$CVaR_{95}[C]$ (B)
Minimum time	87	75	87.1	93.7	1,191,588.30	1,212,083.70	1,217,165.30
Optimal price	8	514	600	600	113,957.20	115,999.30	117,556.30
Equilibrium point	45	308	366.5	379.1	618,670.50	629,362.30	632,750.40

Material Classification and Value-Loss-Aware Allocation Improvement

In view of the problems identified in the original model, we propose an improved allocation strategy based on material classification and risk-sensitive value loss. On the premise that the overall rocket share remains

unchanged, material classification is introduced to prioritize the allocation of high-value and high-sensitivity materials to more robust transportation channels, thereby reducing actual resource losses.

Step1: Resource Typology and Classification Principles

Facing resource usage constraints and demand in actual construction, the rational allocation of 100 million tons of resources is a critical step. Compared with studies on the Apollo program, the International Space Station, and other early lunar bases, structural materials are often the dominant component of initial mass. Referring to space engineering experience, we classify resources according to functional role, transport-related physical attributes, and construction time stage, and divide them into four categories:

A: bulk structural materials (large volume);

B: key equipment (medium weight but sensitive to value loss and delivery delay);

C: consumables and spare parts (light weight but requiring repeated and continuous supply);

D: dangerous and special goods (small quantity but subject to high constraints and high risk).

The proportion of each material category is illustrated in Figure 4. We then introduce the value density V_k ($/kg) and the risk sensitivity coefficient α (dimensionless) for each category to characterize the consequences of failure. Owing to severe hazards such as explosions associated with Class D accidents, safety constraints are imposed: Class D dangerous goods are required to be transported by rockets only.

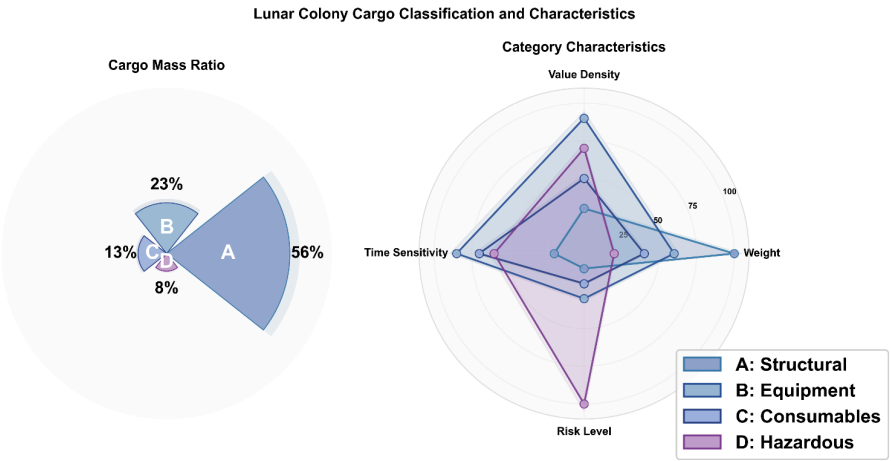

Figure 4. Lunar colony cargo classification and characteristics

Step2: Value Loss Modeling and Risk-Aware Optimization

We divide the total demand M into M_k according to the category $k \in \{A, B, C, D\}$, and define the decision variable $x_k \in [0, 1]$ as the proportion of rocket transportation for category k . Accordingly, $M_{R,k} = x_k M_k$

and $M_{E,k} = (1 - x_k)M_k$. Under the model of continuing Time-Expanded Linear Programming Mixed Transportation Model, under scenario ω , the value loss due to rocket failure is defined as:

$$VL_R = \sum_k \sum_t \left(M_{R,k}^{try}(t) - \Delta M_{R,k}(t) \right) \cdot 1000 \cdot v_k \cdot \alpha_k / 10^9 \tag{23}$$

When the elevator is shut down by a disaster, we approximate the in-transit loss using "one month of elevator throughput" as follows:

$$VL_E^{\omega} = \sum_{t_c \in Y_c^{\omega}} \sum_k \left(\frac{C_E^{\omega}(t_c)}{12} \theta_k \right) \cdot 1000 \cdot v_k \cdot \alpha_k / 10^9, \theta_k = \frac{M_{E,k}}{\sum_j M_{E,j}} \tag{24}$$

Finally, the improved risk model is obtained:

$$\begin{aligned} \mathrm{TotalCost}_{\mathrm{risk}} = \sum_{i=A}^{D} \Bigg[& \left(\frac{Q_i^{\mathrm{rocket}}}{\eta_{\mathrm{rocket}}} \cdot C_{\mathrm{rocket}} + Q_i^{\mathrm{elev}} \cdot C_{\mathrm{elev}} \right) \\ & + \underbrace{\left(\frac{Q_i^{\mathrm{rocket}}}{\eta_{\mathrm{rocket}}} \cdot (1 - \eta_{\mathrm{rocket}}) \cdot V_i \cdot \phi_i \right)}_{\mathrm{ExpectedRocketValueLoss}} \Bigg] \\ & + \underbrace{N_{\mathrm{cut}} \cdot \left(C_{\mathrm{repair}} + \mathrm{Loss}_{\mathrm{transit}} \right)}_{\mathrm{ElevatorCatastropheRisk}} \end{aligned} \tag{25}$$

Step3: Reassessment Results of the Improved Risk Model

Using the improved risk model, we re-evaluated the risk to obtain the rocket transportation data after material classification and compared the model results before and after improvement. By calculating the expected value, we obtained the changes in value loss reduction and risk adjustment cost. Specifically, as shown in the figures, after implementing the material classification optimization, resource allocation under each scenario becomes more targeted. In particular, under the balanced plan, high-value equipment (Class B) and consumables (Class C) are entirely shifted to elevator transportation (with the rocket proportion reduced to 0%), while only the mandatory rocket constraints for hazardous materials (Class D) and a portion of structural materials (Class A, 66.1%) are retained.

This strategy adjustment yields significant risk reduction benefits. The expected value loss $E[VL]$ of the shortest construction-period scheme decreases from \$8255B to \$5438B, representing a reduction of 34.1%. The value loss of the lowest-cost scheme is also reduced by 32.0%. Moreover, the balanced scheme achieves the most pronounced improvement, with its expected value loss reduced from \$5184B to \$1680B, corresponding to a Value-at-Risk stop-loss effect of up to 67.6%. These results strongly demonstrate the effectiveness of the classified diversion strategy in enhancing overall project robustness. Cargo allocation strategy: uniform vs category-optimized is shown in figure 5. Expected value loss improvement comparison is shown in figure 6.

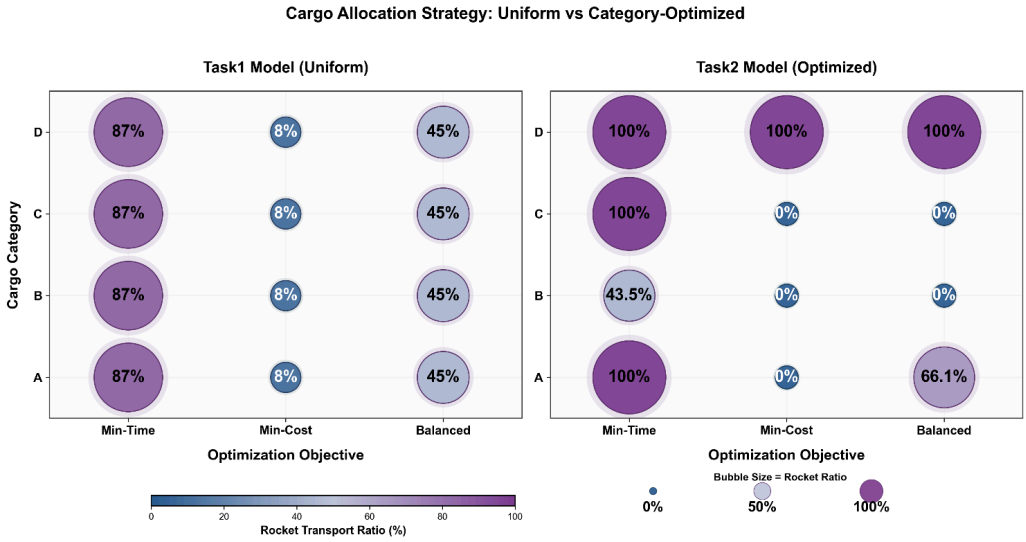

Figure 5. Cargo allocation strategy: uniform vs category-optimized

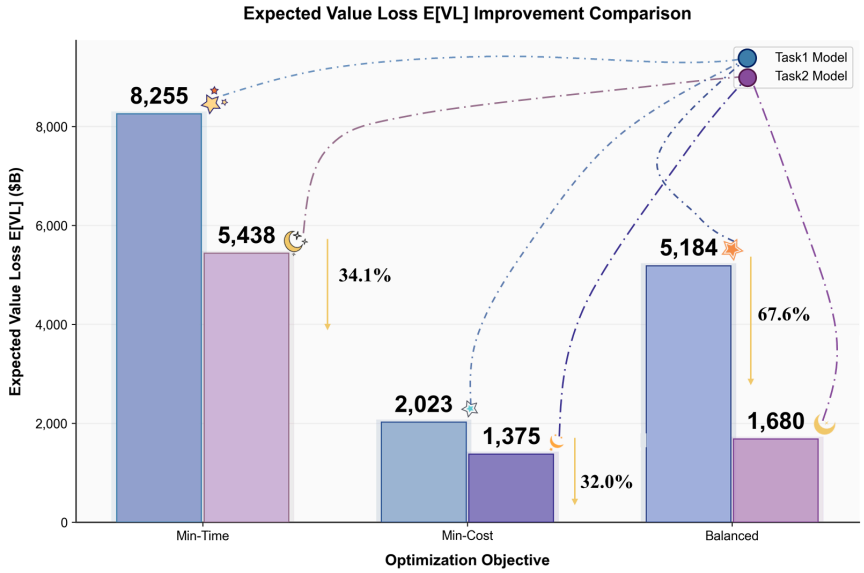

Figure 6. Expected value loss improvement comparison

Operational Water Demand and Inventory-Based Supply Modeling

After the lunar colony enters the full operation stage with a population of 100,000, the issue of water supply shifts from simple "daily consumption" to a critical life-support system problem. It is therefore necessary not only to estimate the annual scale of water use, but also to address a core question: how to ensure continuous water supply within a year, and how to quantify the required transportation channels, additional costs, and executable timelines for this purpose.

Establishment of water recharge model

Establishing a guarantee model to determine the net water supply after the lunar colony enters the full operation stage with a population of 100,000 is a key step. Because daily water budgets differ across age groups, it is particularly important to quantify the daily water demand of different age groups and the population composition of the lunar settlement.

(1) Water demand caliber and annual scale estimation during operation period

By collecting the daily water budget conservation table from NASA BVAD and the data on adequate intake (AI), we find that the daily water budget of space operators under high-intensity conditions is significantly higher than that of ordinary residents. Accordingly, the population is divided into two categories: Category A for astronauts and Category B for residents, and their daily water consumption is summarized as follows. Daily water budget by population group is shown in table 6.

Table 6. Daily water budget by population group

Population Group	Total Water Input (a)	Liquid Water Output (a)	Respiration + Sweat Vapor (a)
Children 1–3 years	1.552	0.758	0.794
Children 4–8 years	2.023	0.987	1.036
Youth 9–13 years	2.608	1.274	1.336
Adolescents 14–18 years	3.038	1.483	1.555
Adults 19–50 years	3.498	1.707	1.790
Middle-aged and Elderly 51–70 years	3.350	1.636	1.714
Elderly > 70 years	3.080	1.505	1.576
Category A - Aerospace Operators	4.467	1.521	2.946

At the same time, we consult global age structure data and its long-term projections from the Handbook of Statistics of the United Nations Conference on Trade and Development (UNCTAD), which are used to describe the population pyramid of "land-like cities" in the mature stage. The data indicates that by 2050,

the proportion of people aged 65 and above will rise to approximately 16%, the proportion of children will continue to decline, and the proportion of the working-age population will remain relatively stable. Therefore, we simulate and divide the population composition of the lunar base according to the proportion of the Earth's population. Combined with the operational and maintenance requirements of the base, a separate list of Category A aerospace operators is defined (set at 0.5%), while the remaining population is classified as Category B residents grouped by age. The resulting population division is shown in Figure 7.

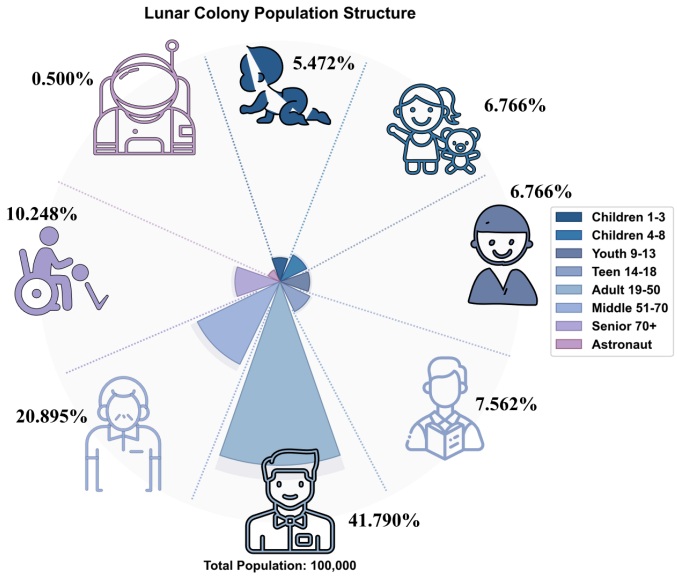

Figure 7. Lunar colony population structure

Considering the operation and water recovery system during the operation period of the base, we further define the total water w^{gross} on the basis of drinking water, we add the operation load of non drinking water but water demand (collectively referred to as other use) such as sanitation, medical treatment, operation and maintenance, public service, etc., so as to form the full use water load during the operation period. For any group g , to maintain vital functions, the daily water budget should be roughly balanced:

$$W_{in,g} = W_{pot,g} + W_{food,g} + W_{met,g}, W_{out,g} = W_{urine,g} + W_{feces,g} + W_{vap,g}, W_{in,g} \approx W_{out,g} \quad (26)$$

We then aggregate the population weights to the total population of the base. Assuming that the population size of group g (including Category A) is P_g and its gross daily water demand is w_g , the total annual water consumption of the base (T/a) is calculated and the total daily per-capita water consumption obtained from our model is 10.5868 L/person/day, which corresponds to an annual total of $W_{gross} = 27,049$ tons/year. This

estimated figure of 10.5868 L per person per day primarily represents the minimum net consumption required to sustain basic human physiological metabolism and basic hygiene. In actual urban operations, industrial, medical, and public service sectors consume vast amounts of water through recycling, but this model assumes that this portion is offset by highly efficient internal closed-loop recycling systems (such as an advanced version of the ECLSS); therefore, only the net loss requiring periodic external replenishment is accounted for here. Finally, the water cycle is incorporated into the annual net water replenishment. NASA reports that the ISS ECLSS has achieved approximately 98% water recovery capacity. However, to ensure sufficient water supply for the lunar base, we set the recovery rate η to 95% and the unrecoverable loss rate ρ (representing net losses due to concentrated brine disposal, pollution scrapping, leakage, etc.) to 2%. Therefore, the annual net water replenishment required from external transportation is:

$$W_{makeup} = (1 - \eta + \rho)W_{gross} \tag{27}$$

(2) Establishment of Water Supply Model

Assuming that the unit freight costs of the elevator and rocket are c_E, c_R , respectively, the transportation costs associated with the annual net water replenishment W_{makeup} are given by:

$$J_E = c_E \cdot 1000 W_{makeup}, J_R = c_R \cdot 1000 W_{makeup} \tag{28}$$

We convert the time scale to months $(m = 1, ..., 12)$. Accordingly, the annual demand is expanded into monthly demand:

$$D_m^{water} = \frac{days_m}{365} W_{makeup} \tag{29}$$

And a rigid monthly demand constraint is imposed:

$$x_m^{E,water} + x_m^{R,water} \geq D_m^{water} \tag{30}$$

Therefore, the annual additional cost ΔJ and the equivalent number of elevator operation days T_E^{water} required to ensure water supply are obtained as:

$$\Delta J = J^*\left(D^{base} + D^{water}\right) - J^*\left(D^{base}\right) \tag{31}$$

The corresponding utilization ratio and equivalent operation time of the elevator are defined as:

$$Util_E^{water} = \frac{X_E^{water}}{C_E^{eff}}, T_E^{water} = 365 \cdot Util_E^{water} \tag{32}$$

This formulation yields the additional cost and timeline required to ensure sufficient water supply for one consecutive year. As illustrated in Figure 8, panel (a) shows that the monthly delivery volume exhibits high stability, while panel (b) further demonstrates the significant cost-control advantage of the water recharge model.

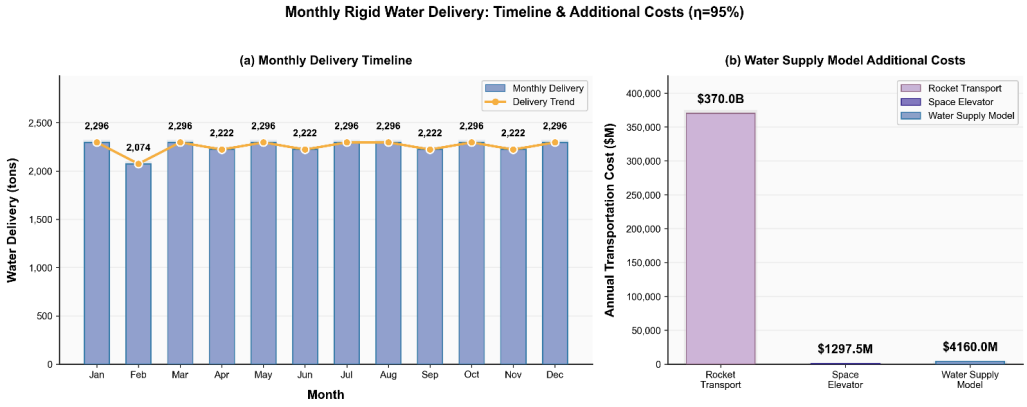

Figure 8. Monthly rigid water delivery: timeline & additional costs (n=95%)

Environmental Impact Assessment

With a water recovery rate of 95%, the base still faces an annual net water replenishment demand of approximately 27,031 tons. This substantial material gap must be supplied through the Earth Moon transportation system. Whether relying on traditional chemical rockets or future space elevators, the stability of the supply chain is directly linked to Earths environmental burden. Therefore, under the premise of satisfying the survival reliability requirements of the base, we further optimize the transportation strategy to identify the scheme with the minimum environmental cost.

Scenario definition: ideal technology and realistic risk

According to the technical specifications of the Space Elevator System, the elevator lifting subsystem is powered by advanced clean energy and can operate with net-zero atmospheric emissions, without thermal pollution. Under normal conditions, this implies a near-zero marginal environmental cost for elevator-based transportation. However, net-zero does not mean zero risk. Because routine operations are environmentally benign, the dominant source of environmental impact arises from system unreliability. When faults—such as tether vibrations or debris-avoidance maneuvers—interrupt elevator operations and lead to inventory depletion, the system is forced to revert to the highly polluting rocket-based transportation mode.

Environmental Impact Assessment Model Formulation

To quantify the above risks, we establish an environmental impact function E_{total} driven by the supply chain strategy. Since the elevator itself operates at net zero emissions, we focus on the probabilistic accumulation of emergency damage, which consists of two components: the normalized environmental burden from infrastructure operation and maintenance, and the impact caused by sudden emergency launches.

$$E_{\text{total}} = \underbrace{\sum_{i=1}^{N_{\text{launch}}} \left(E_{\text{CO2}}^{\text{rocket}} + \alpha \cdot E_{\text{O}_3} + \beta \cdot E_{\text{debris}} \right)}_{\text{Environmental damage caused by emergency launch}} + \underbrace{E_{\text{residual}}}_{\text{Rigid emissions from infrastructure}} \tag{33}$$

Because rockets and elevators are both used for material transportation in most scenarios, safety stock becomes an important factor in assessing the environmental impact of the transportation system. Our objective is to identify the environmental optimal inventory strategy s* that minimizes the expected total environmental impact while satisfying the base service-level constraint (water shortage probability $P_{shortage} \approx 0$):

$$\min_{s} E[E_{total}(s)] \quad s.t. \quad P_{shortage}(s) \leq \varepsilon \tag{34}$$

Result analysis and optimization

(1) Coupled Effects of Supply Chain Vulnerability and Environmental Costs

In the context of full operation of the lunar migration base, we use Monte Carlo method to carry out 10000 iterations under different resource inventory scenarios. The results are shown in the figure of the relationship

between safety stock and environmental impact. There is a profound nonlinear coupling relationship between inventory strategy and environmental impact.

• Step1: Environmental shock under low inventory (s=15 days)

When the safety stock is set to 15 days, the water recharge model exhibits a high level of environmental pollution. Simulation results indicate that, under this strategy, an average of 3.1 emergency rocket launches is required per year. This not only results in 518.9 tons of pollutant gas emissions annually, but, more importantly, emergency rocket launches are themselves associated with high operational risk and strict launch window constraints. Frequent emergency launches therefore continuously challenge the environmental baseline of the Earth system. The inventory-environment curve is shown in figure 9.

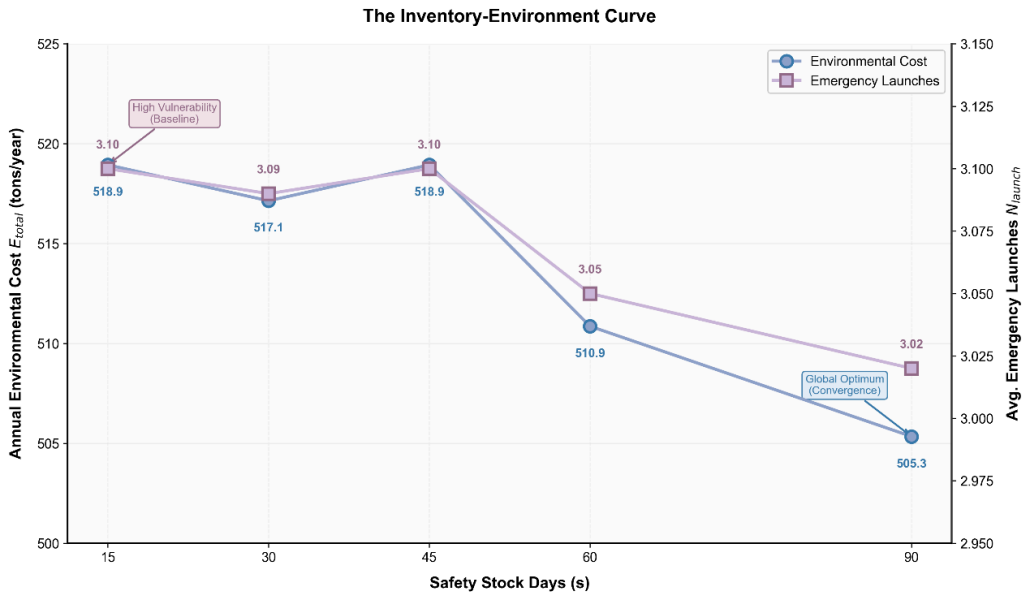

Figure 9. The inventory-environment curve

Step2: Green smoothing effect under high inventory (s≥60 days)

With the increase of safety stock, the environmental impact curve shows an obvious marginal decreasing effect. Inventory essentially acts as a low-pass filter, successfully filtering out the high-frequency elevator fault interference, so that most supply interruptions can be digested by consuming inventory within the base without disturbing the emergency system on the earth side.

(2) optimization strategy: Exchange “space” for “environment”

Building on the quantified relationship between safety stock and environmental impact, we incorporate material inventory as a key decision variable in the replenishment model. This strategy reflects a trade-off:

maintaining an additional 75 days of water reserves (≈5,600 tons) requires extra capital and maintenance expenditures for storage infrastructure. In return, the policy satisfies residents' water demand while reducing the probability of emergency rocket launches toward its theoretical minimum. Therefore, inventory sizing is not merely a logistics decision but also an environmental one. In the Space Elevator System era, the largest warehouse can function as the most effective environmental safeguard, because it suppresses the need for rocket intervention in the supply chain.

CONCLUSIONS

This study systematically addresses path optimization, risk management, and long-term resource assurance challenges in large-scale logistics by constructing an integrated computational framework combining trend forecasting, linear programming, and stochastic simulation. It demonstrates the superior performance of hybrid collaborative architectures in handling extreme logistics demands. The research not only provides robust material allocation algorithms but also quantifies the core value of inventory strategies in enhancing system environmental resilience. However, the model simplifies certain variables during construction—for instance, assuming unit transportation costs remain approximately linear across channels—failing to fully capture nonlinear economies of scale or complex market game dynamics under hyper-scale conditions. Furthermore, current stochastic simulations primarily rely on predefined probability distributions, with room for improvement in dynamic learning capabilities regarding sudden "black swan" events. Future research should focus on integrating reinforcement learning algorithms for real-time adaptive scheduling and exploring the use of digital twin technology with real-time feedback from physical sensors to build intelligent logistics hubs capable of proactive fault detection and predictive maintenance.

Author Contributions

Conceptualization, J.Z. and J.H.; methodology, J.Z. and J.H.; software, C.X.; validation, J.Z. and C.X.; formal analysis, J.H.; investigation, C.X.; resources, J.Z.; data curation, J.H.; writing—original draft preparation, J.Z. and J.H.; writing—review and editing, J.Z. and C.X.; visualization, J.H.; supervision, J.Z.; project administration, C.X. All authors have read and agreed to the published version of the manuscript.

Conflicts of Interest

The authors declare no conflict of interest.

Funding

This research received no external funding.

Acknowledgements

Not applicable.

REFERENCES

[1] Space Exploration Technologies Corp (SpaceX). Falcon Payload User's Guide. 2025. https://spacex.com.pl/files/2017-10/falcon-9-users-guide-rev-2.0.pdf?4f8d2248dc

[2] Federal Aviation Administration (FAA), Office of Commercial Space Transportation. SpaceX Falcon Program Final Environmental Assessment (EA) and Finding of No Significant Impact (FONSI). Washington, D.C.: FAA. https://www.faa.gov/space

[3] U.S. Energy Information Administration (EIA). Electricity Sales, Revenue, and Average Price. https://www.eia.gov/electricity/sales_revenue_price/

[4] Lynch CS, Goodliff KE, Stromgren C, Vega J, Ewert MK. Logistics Rates and Assumptions for Future Human Spaceflight Missions Beyond LEO (V5). NASA (NTRS). 2023. https://ntrs.nasa.gov/api/citations/20230012635/downloads/Logistics%20Rates%20and%20Assumptions%20Beyond%20LEO%20V5.pdf

[5] Ewert MK, Chen TT, Powell CD. Life Support Baseline Values and Assumptions Document (BVAD), Rev. 2 (Final). NASA (NTRS). 2022. https://ntrs.nasa.gov/api/citations/20210024855/downloads/BVAD_2.15.22-final.pdf

[6] NASA Office of the Chief Health & Medical Officer (OCHMO). OCHMO Technical Brief: Water—Human Consumption (OCHMO-TB-027). 2023. https://www.nasa.gov/ochmo/

[7] National Academies of Sciences, Engineering, and Medicine. Dietary Reference Intakes for Water, Potassium, Sodium, Chloride, and Sulfate. Washington, DC: The National Academies Press. 2005. doi: 10.17226/10925.

[8] United Nations, Department of Economic and Social Affairs, Population Division. World Population Prospects 2024: Summary of Results. https://population.un.org/wpp/

[9] U.S. Environmental Protection Agency (EPA). Emissions & Generation Resource Integrated Database (eGRID). https://www.epa.gov/egrid

[10] Roncoli RB. Lunar Constants and Models Document. JPL Technical Document D-32296. 2020. https://www.scirp.org/reference/referencespapers?referenceid=214247

[11] Huang J, Hu W, Tian Y, Yin L, Zhang H, Wang G. Synergistic modification of Sn-9Zn solder using nano-SiC-based interface-active multifunctional reinforcements. Materials Characterization. 2025; 230(PB): 115784-115784. doi: 10.1016/J.MATCHAR.2025.115784.

[12] Cui L, Chu H, Wang J, Guo W, Yang F, Hu Z. Collaborative path optimization model of power material supply chain based on hash index spatio-temporal graph neural network. Array. 2025; 28: 100598-100598. doi: 10.1016/J.ARRAY.2025.100598.

[13] Michael AS, Atieh MA, Nkwocha E, Rawashdeh NA. Cyber-physical framework for smart paint manufacturing: Hybrid integration of PLC and recipe management simulation. Advances in Mechanical Engineering. 2025; 17(12). doi: 10.1177/16878132251406501.

[14] Sengul AM, Aras AA. A geoarchaeological analysis on the identification and origin of volcanic rocks used in monumental architectures in Ayanis city. Journal of Archaeological Science: Reports. 2026; 69: 105489-105489. doi: 10.1016/J.JASREP.2025.105489.

[15] Fliegner JF. The weakest link? A spatial planning perspective on supply chain and resilience risks for Europe's offshore wind ambitions. Energy Policy. 2026; 209(PA): 114970-114970. doi: 10.1016/J.ENPOL.2025.114970.

[16] O'Connor L. A comparative review of material supply chains and sustainability pathways in steel and battery technologies. The Extractive Industries and Society. 2026; 25: 101814-101814. doi: 10.1016/J.EXIS.2025.101814.

[17] Li H, Cui Z, Chen Y, Tang W. Reusable Fe3O4MSiO2 contact-electro-catalysis for recycling valuable metal from spent lithium-ion batteries. Chemical Engineering Science. 2026; 320(PA): 122350-122350. doi: 10.1016/j.ces.2025.122350.

[18] Kim H, Kim S, Lee J, Jeong K, Hong T, An J. Development of a blockchain-based platform for real-time carbon emission assessment of building material supply chain. Building and Environment. 2026; 287(PB): 113907-113907. doi: 10.1016/J.BUILDENV.2025.113907.

[19] Zhang Y, Wang Y, Liang Y, Wang K, Zhang H. Demand-side strategies can mitigate critical material supply bottlenecks in China's solar photovoltaic deployment: A dynamic integrated assessment framework. Sustainable Production and Consumption. 2025; 61: 48-65. doi: 10.1016/J.SPC.2025.10.005.